# JCB

## Article

# The protein storage vacuole: a unique compound organelle

Liwen Jiang,[1] Thomas E. Phillips,[2] Christopher A. Hamm,[3] Yolanda M. Drozdowicz,[4] Philip A. Rea,[4] Masayoshi Maeshima,[5] Sally W. Rogers,[3] and John C. Rogers[3]

[1]Department of Biology, The Chinese University of Hong Kong, Shatin, New Territories, Hong Kong, China
[2]Division of Biological Sciences, University of Missouri, Columbia, MO 65211
[3]Institute of Biological Chemistry, Washington State University, Pullman, WA 99164
[4]Plant Science Institute, Department of Biology, University of Pennsylvania, Philadelphia, PA 19104
[5]Graduate School of Bioagricultural Science, Nagoya University, Chikusa-ku, Nagoya 464-8601, Japan

Storage proteins are deposited into protein storage vacuoles (PSVs) during plant seed development and maturation and stably accumulate to high levels; subsequently, during germination the storage proteins are rapidly degraded to provide nutrients for use by the embryo. Here, we show that a PSV has within it a membrane-bound compartment containing crystals of phytic acid and proteins that are characteristic of a lytic vacuole. This compound organization, a vacuole within a vacuole whereby storage functions are separated from lytic functions, has not been described previously for organelles within the secretory pathway of eukaryotic cells. The partitioning of storage and lytic functions within the same vacuole may reflect the need to keep the functions separate during seed development and maturation and yet provide a ready source of digestive enzymes to initiate degradative processes early in germination.

## Introduction

In plant cells, protein storage vacuoles (PSVs)* and lytic vacuoles (LVs) represent separate organelles because they are served by distinct transport vesicles (Hinz et al., 1999), and their membranes are marked by the presence of different tonoplast intrinsic proteins (TIPs): α-TIP plus δ-TIP for PSVs and γ-TIP for LVs (Hoh et al., 1995; Paris et al., 1996; Jauh et al., 1999). PSVs in most seeds contain three morphologically distinct regions: the matrix, crystalloid, and globoid (Lott, 1980; Weber and Neumann, 1980). The matrix and crystalloid were known to contain storage proteins, whereas the globoid was comprised of phytic acid crystals (Lott, 1980; Weber and Neumann, 1980). Globoid "cavities" were considered morphological artifacts, resulting from loss of the crystals during tissue preparation for microscopy (Lott, 1980; Weber and Neumann, 1980). These morpho-

logically defined components were thought to result from assembly of soluble molecules after they were mixed together within one vacuole lumen.

However, recently we demonstrated that the matrix is a destination of soluble proteins, but the PSV crystalloid additionally contains integral membrane proteins and substantial amounts of lipid (Jiang et al., 2000). This membrane-containing internal structure results from uptake of cytoplasmic prevacuolar organelles, termed dark intrinsic protein (DIP) organelles (Jiang et al., 2000), that are likely to be equivalent to precursor-accumulating (PAC) vesicles characterized from developing pumpkin and castor bean seeds (Hara-Nishimura et al., 1998). These prevacuolar organelles receive protein traffic directly from the ER and via the Golgi complex (Hara-Nishimura et al., 1998; Jiang et al., 2000). In addition to the condensed appearing osmiophilic contents that assemble into the PSV crystalloid, the prevacuolar organelles also contain internal vesicles (Hara-Nishimura et al., 1998; Jiang et al., 2000). In PAC vesicles, indirect evidence indicates that the internal vesicles may contain proteins trafficking from the Golgi complex (Hara-Nishimura et al., 1998). Thus, uptake of the organelles into the PSV would also result in uptake of internal vesicles that are likely to have a fate separate from components assembled into the crystalloid.

Here, we demonstrate that the globoid cavity is defined by a unit membrane. This membrane is specifically marked by

the presence of vacuolar H$^+$-pyrophosphatase (V-PPase) and γ-TIP. In transgenic plants expressing a chimeric integral membrane reporter protein (designated Re-F-B-B) that traffics to the lytic prevacuolar compartment where it is processed proteolytically (Jiang and Rogers, 1998), the globoid cavity contains the processed form of the reporter protein. Additionally, as assessed in wild-type plants the globoid cavity contains a tobacco protein closely related to the barley cysteine protease aleurain. Thus, it has integral membrane and soluble markers characteristic of an LV.

In most plant cells, as far as is known, LVs and vacuoles that have characteristics of PSVs are separate structures (Di Sansebastiano et al., 1998, 2001), and trafficking pathways to them utilize prevacuolar compartments that also are distinct (Jiang and Rogers, 1998). However, in specific cells where the complex type of PSV formation as described here occurs, predominantly in the seed embryo but also in certain root tip cells, Re-F-B-B traffics through the cytoplasmic prevacuolar DIP organelles/PAC vesicles where it is also present in proteolytically processed form; these same organelles also contain membrane proteins that are destined for the PSV crystalloid. This result indicates that proteins within the prevacuolar organelles destined for the PSV globoid are partitioned away from proteins destined for the PSV storage compartment and provides the basis for a model by which a globoid compartment and its contents could be assembled within the developing PSV.

## Results

### A globoid cavity membrane

Our previous results indicated that the PSV crystalloid was formed when membrane-containing internal structures from prevacuolar organelles were taken up by the developing vacuole. This demonstration of internal membranes within storage vacuoles raised the question as to whether the globoid was a separate compartment defined by its own membrane. There is a strong precedent for storage of crystals within membrane-bound compartments inside vacuoles: calcium oxalate crystals in vacuoles are contained within crystal

Figure 1.  **A unit membrane surrounds the globoid cavity.** (A and B) Sections from tobacco seeds treated with 0.5% permanganate where thin sections were counter stained with uranyl acetate and lead citrate. Insets show lower magnification images of PSVs from dry tobacco seeds where the globoid cavity and crystalloid are indicated with G and C, respectively, and L indicates lipid in oil bodies adjacent to the PSV. Arrows indicate examples of unit membrane appearance. (C) Tonoplast from sections as in the A and B; the scale bar is positioned over a globoid cavity, and L indicates oil bodies outside the PSV. (D) Section from a tobacco seed treated with 2.5% permanganate where thin sections were not counterstained. L and G as in A and B; note staining that appears to demonstrate internal structures within the oil bodies adjacent to L. (E) Enlargement of globoid cavity labeled with G in D. Arrows indicate examples of unit membrane appearance. Bars, 200 nm.
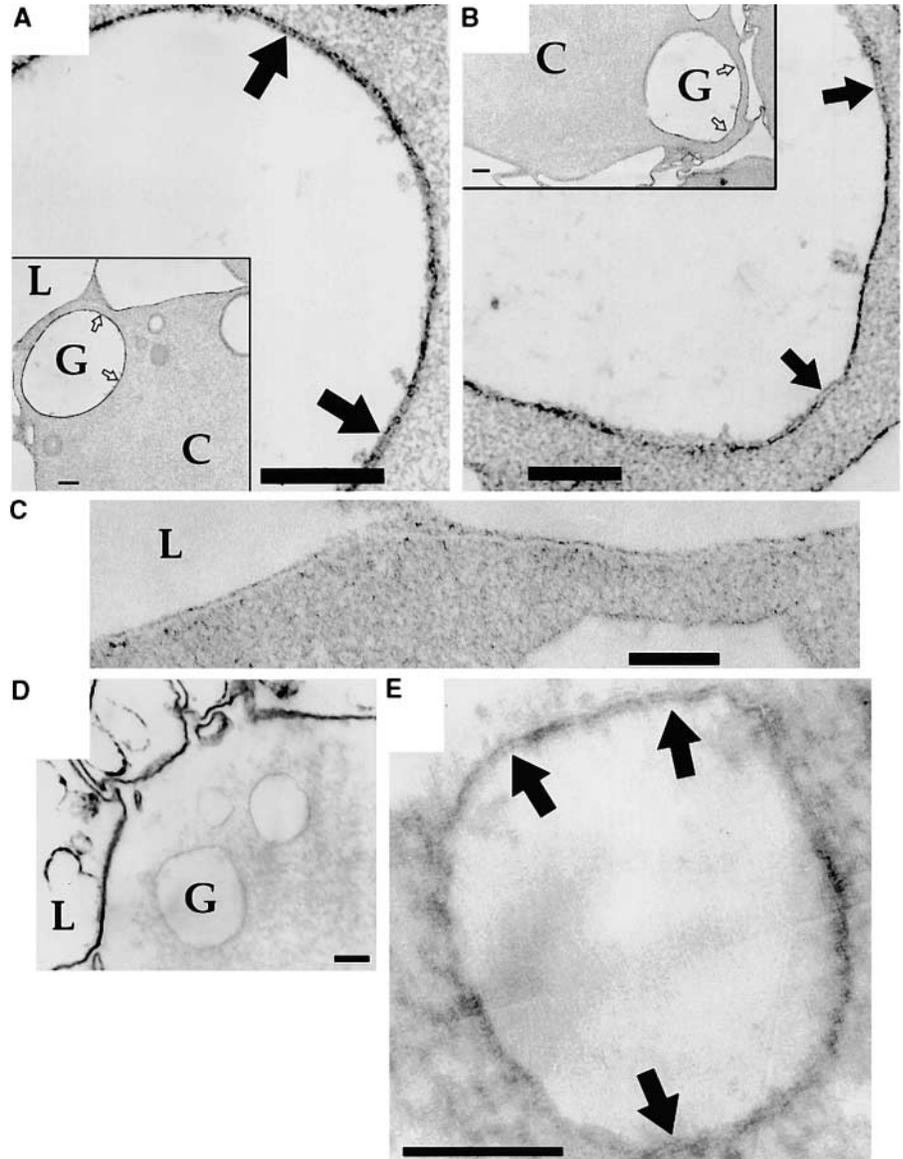
chambers defined by structures having the classic appearance of unit membranes (Arnott and Pautard, 1970; Franceschi, 1984). Demonstration of unit membranes in some of those studies was facilitated by treatment of the plant tissues with permanganate, which reacts specifically with phospholipids (Ongun et al., 1968; Meek, 1976) because this strongly oxidizing compound extracted the crystal contents and much protein that otherwise obscured the membranes' morphology (Arnott and Pautard, 1970). Therefore, we used a similar protocol to prepare mature tobacco seeds for transmission EM study.

In PSVs from tissue treated with 0.5% permanganate, the globoid crystals had been removed by permanganate treatment, and globoid cavities were identified readily by their content of numerous wisps of flocculent-appearing material that were not present in the lipid spaces surrounding the PSVs (Fig. 1, A and B, insets). These cavities were defined by an electron-dense border, which when cut perpendicularly demonstrated the appearance typical of a unit membrane (Fig. 1, A and B, arrows). Permanganate fixation is known to result in a granular appearance on membranes; this granularity is evident both on the globoid membranes and the PSV tonoplast (Fig. 1 C). To exclude the possibility that the unit membrane appearance shown in Fig. 1, A and B, was due to an artifact of stain deposited on both sides of the thin sections, sections of tissue treated with 2.5% permanganate were viewed without additional staining. Thus, any electron density of structures would result from labeling by permanganate and bismuth exposure before the tissue was embedded. Treatment with the higher permanganate concentration resulted in heavy labeling of the surface of oil bodies surrounding PSVs and loss of a visible PSV tonoplast; however, an electron-dense boundary around globoid cavities was still present (Fig. 1 D). When viewed at higher magnification, it is evident that this boundary retains a unit membrane appearance (Fig. 1 E, arrows). These results strongly support the concept that the globoid cavity is defined by a membrane.

### Association of V-PPase with the globoid cavity membrane

To investigate the nature of a globoid membrane, we used confocal immunofluorescence to localize different integral membrane proteins within PSVs. Initial studies focused on V-PPase. The studies used four different antisera: one raised to purified mung bean V-PPase (Maeshima and Yoshida, 1989) and three different antisera raised to synthetic peptides representing different sequences within V-PPase molecules, 1401, 1368, and 324.

In PSVs in mature tomato embryos, the globoid is particularly prominent and can be identified readily as a large round structure protruding from one end of the PSV (Spitzer and Lott, 1980) (Fig. 2 A). Electron microscopic thin-section and freeze-fracture studies have demonstrated that the globoid is contained entirely within the PSV (Lott, 1980; Spitzer and Lott, 1980). When studied by wide-field immunofluorescence, the PSV tonoplast labeled for α-TIP, whereas the globoids were outlined by labeling for V-PPase (Fig. 2, A and B). To determine how frequently V-PPase labeling coincided with structures having the appearance of

globoids, we used confocal immunofluorescence and obtained multiple optical sections that were analyzed by superimposing pixels representing specific fluorescence on visible wavelength images that were collected concurrently with the fluorescent images. An example is presented in Fig. 2 C. On the right is a visible image where solid arrows indicate globoids that had fluorescent labeling in at least one optical section, and arrowheads indicate globoids that were not labeled. To the left is the same image with immunofluorescence pixels superimposed. In two collections of images comprising 4 and 6 optical sections, respectively, 90% of the globoids were labeled. Thus, most structures morphologically identified as globoids labeled with antibodies raised to the purified V-PPase protein. We then used a matrix marker antibody to define the PSV matrix and thereby outline internal spaces defined by globoid (Fig. 2 D, thick arrows) and crystalloid (Fig. 2 D, thin arrows); in double-labeling experiments, V-PPase labeling was clearly on structures within PSVs that were surrounded by matrix (Fig. 2 E). These experiments used both the antiserum raised to purified V-PPase (Fig. 2, A–C) and the 1368 antipeptide antiserum (Fig. 2 E). To further test whether the immunofluorescence labeling observed was specific for V-PPase and not due to cross-reactivity with another protein, we compared labeling obtained with 1368 antiserum to that obtained with the two other antipeptide antisera, 1401 and 324; all antisera colocalized on structures with the appearance characteristic of globoids (Fig. 2, F and G, arrows). These results, where four different antisera each raised to a different set of V-PPase epitopes gave similar labeling patterns, strongly support the conclusion that V-PPase protein is in a membrane surrounding the globoid. The results also indicate that little V-PPase, as detected by the antibodies, is present in the PSV tonoplast in tomato embryos.

### γ-TIP and V-PPase are associated with purified globoids

To further test the association of V-PPase and globoid cavities, we prepared tonoplast, crystalloid, and globoid fractions from PSVs isolated from mature dry tomato seeds. To assess the relative purity of each fraction, 5% of each fraction was electrophoresed on SDS-PAGE, transferred to nitrocellulose, and probed with anti-TIP antibodies; based on our previous results (Jauh et al., 1999; Jiang et al., 2000) and results from immunofluorescence studies presented below, we defined δ-TIP as a marker for PSV tonoplast, DIP for crystalloid, and γ-TIP for globoid. In the results presented in Fig. 3 A, bands recognized by each of the antibody preparation are of a size appropriate for TIPs. As shown in Fig. 3 A, middle, DIP was predominantly in the crystalloid fraction from the standard procedure (lane 2) and in the tonoplast plus crystalloid fraction from the alternate procedure (lane 4) with only a trace in the purified tonoplast fraction (lane 1). Therefore, there was little contamination of either tonoplast or globoid fraction with crystalloid. When δ-TIP was tested (Fig. 3 A, top), approximately equal amounts were present in the tonoplast (lane 1) and crystalloid (lane 2) fractions from the standard procedure with relatively little in either globoid fraction (lanes 3 and 5). In contrast, when γ-TIP was tested (Fig. 3 A, bottom), little was present in the
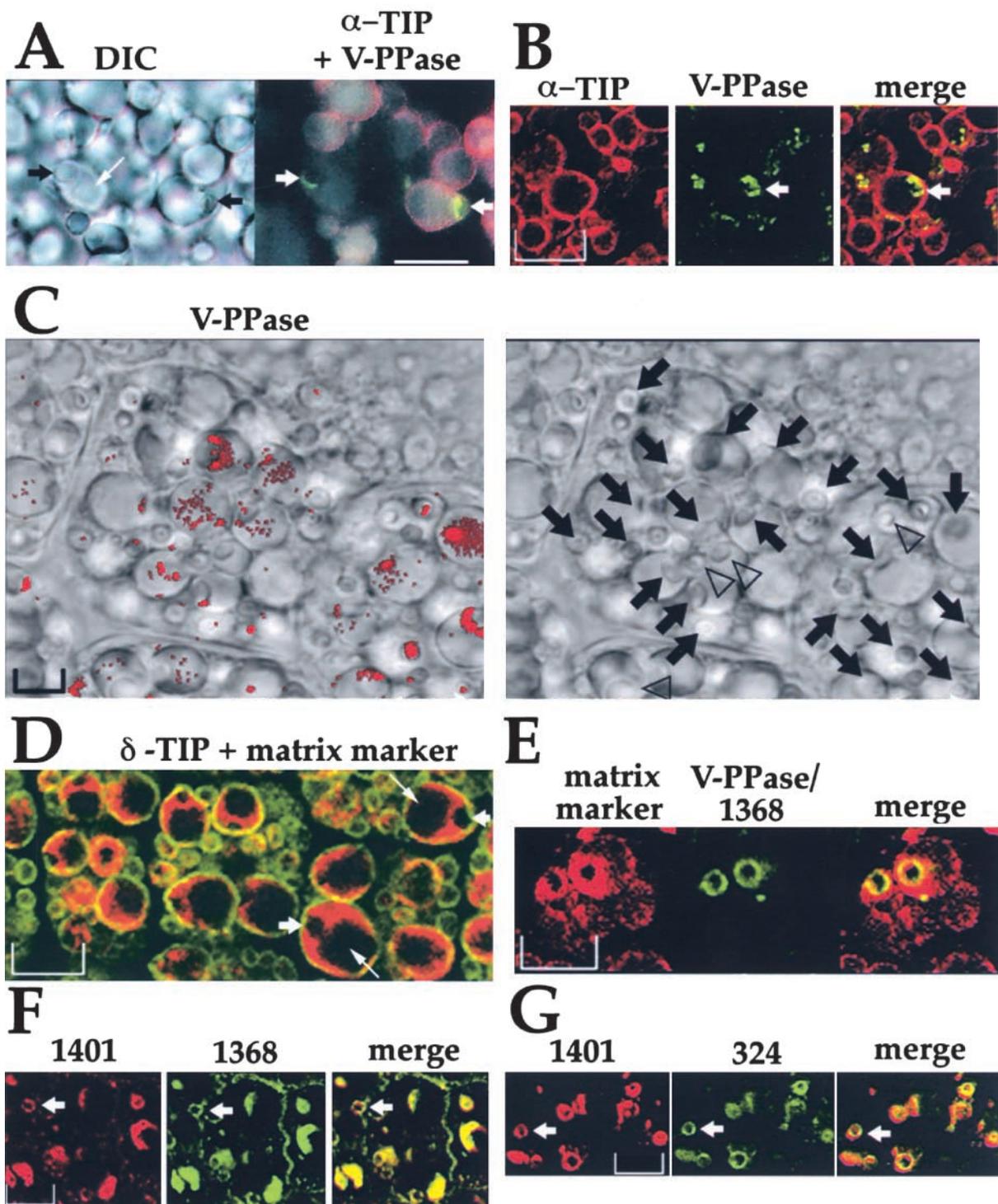
Figure 2.  **Localization of V-PPase in tomato embryo PSVs.** (A) Paraffin section from a mature desiccated seed labeled with anti–V-PPase protein antiserum (FITC; green) and anti–α-TIP MAb38A (rhodamine; red) viewed by differential interference contrast (DIC, left) or wide-field fluorescence (right). Large arrows, globoids; thin arrow, crystalloid. (B) Confocal immunofluorescence of section labeled as in A; arrow, globoid. (C, left) Pixels representing red fluorescence collected from a confocal image of a tomato seed section labeled for V-PPase were superimposed onto a visible light image collected simultaneously with the fluorescent image. (Right) Solid arrows indicate globoids that were seen to be labeled with the antibody in at least one of the several optical sections obtained, whereas open arrowheads indicate globoids that were not labeled. (D) Confocal immunofluorescence of section labeled with anti–δ-TIP (green) and mAb IgM38 matrix marker (red); arrows as in A. (E) Confocal immunofluorescence of section labeled with matrix marker (red) and anti–V-PPase peptide 1368 antiserum (green). (F) Confocal immunofluorescence comparison of anti–V-PPase peptide 1401 (red) and 1368 (green) antisera; colocalization is indicated by yellow in the merged image. (G) Comparison of peptide 1401 and peptide 324 antisera as in E. Bars, 10 μm.
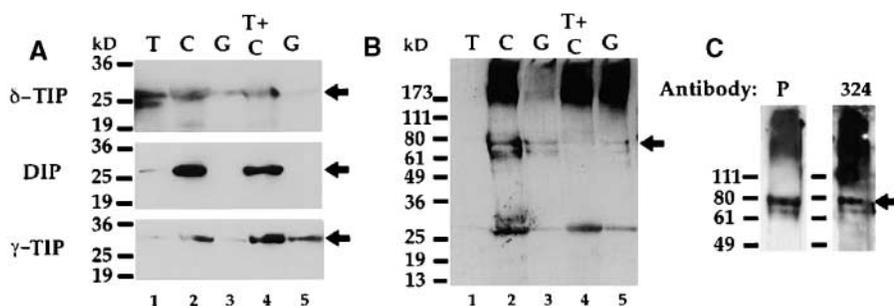
Figure 3. **Immunoblot analysis of fractions obtained from purified tomato PSVs.** (A) Aliquots representing 5% of each fraction were electrophoresed, transferred to nitrocellulose, and probed with anti–δ-TIP (top), anti-DIP (middle), or anti–γ-TIP (bottom) antibodies; arrows, specific labeling of each protein. (B) Immunoblot was probed with anti–V-PPase antibodies. (Arrow) An ∼70-kD dimer of the size expected for V-PPase. (C) Individual strips carrying the globoid fraction proteins were probed with antiserum to V-PPase protein (P) or with anti-324 peptide antiserum; arrow, ∼70-kD dimer recognized by both preparations. T, tonoplast; C, crystalloid; G, globoid; T + C, tonoplast plus crystalloid. Lanes 1–3, standard fractionation procedure; lanes 4 and 5, alternative procedure; numbers to the left in each indicate positions of molecular weight markers in kD.

tonoplast fraction (lane 1), whereas approximately equivalent amounts of protein were present in crystalloid (lane 2), tonoplast plus crystalloid (lane 4), and globoid from the alternative procedure (lane 5). When the patterns obtained for δ- and γ-TIPs are compared using signals obtained in crystalloid-containing fractions for reference, it is evident that δ-TIP was the predominant isoform present in tonoplast, whereas γ-TIP was the predominant isoform present in globoid obtained by the alternative procedure. We hypothesize that the only trace amount of γ-TIP in the globoid prepared from the standard procedure (lane 3) was due to loss of membrane containing the protein during prolonged exposure to an aqueous environment in the sucrose gradient centrifugation step. The presence of both δ- and γ-TIP in the crystalloid and tonoplast plus crystalloid fractions could be due to nonspecific interactions of membrane fragments with crystalloids after the PSVs were lysed.

We then assessed the presence of V-PPase in the same fractions (Fig. 3 B). The antiserum to the purified protein identified a doublet in the ∼70-kD range (Fig. 3B, arrow) in crystalloid (lane 2), globoid (lane 3), and globoid from the alternative procedure (lane 5); an additional band of ∼30 kD was most abundant in crystalloid and tonoplast plus crystalloid fractions. When aliquots of the globoid fraction (lane 3) were rerun and probed with the different anti–V-PPase antisera, 324 labeled a doublet (Fig. 3 C, arrow) that coincided with the doublet detected with the antiserum to the full-length protein (lane P); the ∼30-kD band was not detected by 324 antiserum (unpublished data). We concluded that the two members of the ∼70-kD doublet, a size which is appropriate for V-PPase (Zhen et al., 1997), represent tomato V-PPase proteins, and their presence in globoid fractions supports the specificity of the immunofluorescence results.

## Immunolocalization of γ-TIP to globoid cavity membrane

We sought to characterize the globoid cavity membrane further by identifying other proteins that were localized to it. As noted above, a protein of the appropriate size for a TIP was recognized by our anti–γ-TIP peptide polyclonal antibodies in globoid preparations from tomato seeds. We tested further the specificity of this association with confocal immunofluorescence studies using three different anti–γ-TIP antibody preparations on sections of embryos from seeds from three different plant species, tobacco, tomato, and

snapdragon (*Antirrhinum majus*). Results from tobacco are shown in Fig. 4 where the anti–γ-TIP peptide monoclonal antibody MAb351 was used. In Fig. 4 A, the different symbols point to structures within PSVs having a morphology consistent with globoids (Fig. 3 A, top, left). When labeling for V-PPase (red) was compared with that for γ-TIP (green), both antibodies colocalized on these globoid-like structures as shown in the merged image.

The identity of these structures as globoids was confirmed using electron microscopic immunocytochemistry (Fig. 4 B). This approach was particularly problematic, since the mild fixation and weakly cross-linked embedding resins required for successful immunocytochemistry resulted in poor preservation of the globoids. Furthermore, the electron-dense contents of the globoids tended to migrate during the immunostaining procedure and obscure underlying gold particles. Despite these limitations, MAb351 against γ-TIP was found preferentially associated with the outer margins of globoids in tomato (Fig. 4 B). Morphometric analysis of randomly chosen globoids revealed that within a 30-nm radius of the outer edge of the globoid there were 0.030 ± 0.005 (mean ± S.E.) gold particles per $\mu m^2$ for $n = 18$ globoids. Examination of the tonoplast and crystalloid regions present in the same micrographs showed that within a 30-nm radius of the tonoplast there were only 0.005 ± 0.002 gold particles per $\mu m^2$ and only 0.001 ± 0.0005 gold particles per $\mu m^2$ associated with the crystalloid region. The number of gold particles per $\mu m^2$ associated with the globoid was significantly different ($p < 0.001$) than that found associated with either the tonoplast or crystalloid, but the difference in binding between the crystalloid and tonoplast regions was not significant ($p > 0.1$).

When labeling on sections of embryos from tomato and snapdragon obtained with antiserum raised to purified γ-TIP, VM23 (Maeshima, 1992; Higuchi et al., 1998) was compared with labeling obtained with antiserum to purified V-PPase protein (Fig. 5 A), V-PPase (red), and γ-TIP (green) colocalized on structures within PSVs as demonstrated in the merged image (right). Similar results were obtained using the anti–γ-TIP peptide polyclonal antibodies, although they additionally gave weak tonoplast labeling (unpublished data). Consistent with their location on the globoid membrane, labeling for each protein was separate from labeling with anti-DIP antibodies (Fig. 5 B; DIP is a marker for the PSV crystalloid) (Jiang et al., 2000). The fact that three independently derived
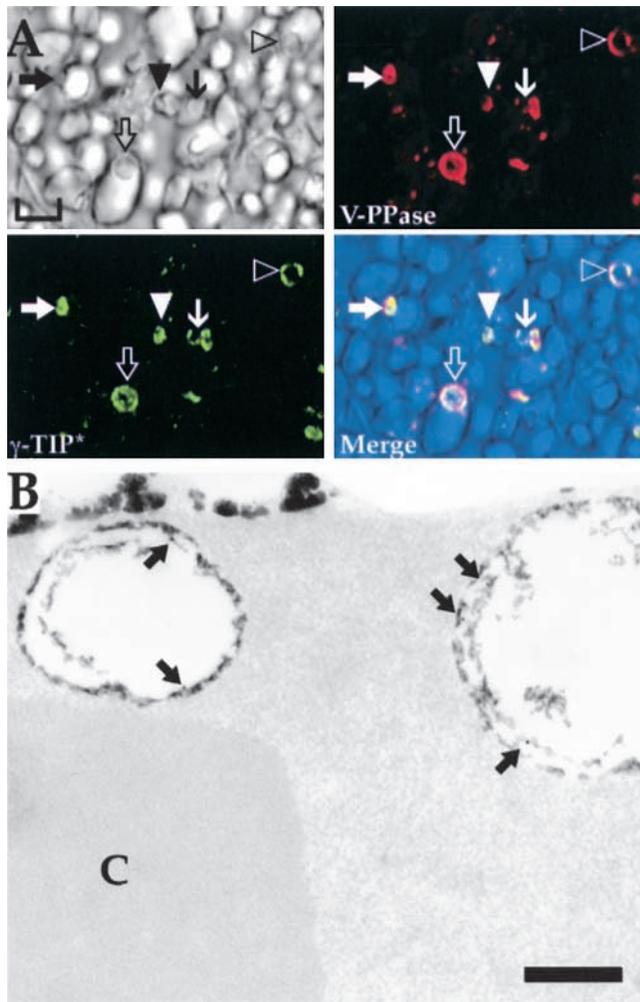
Figure 4.  γ-TIP is associated with globoids. (A) Confocal immunofluorescence images of a tomato seed section labeled with anti–V-PPase protein antiserum (red) and anti–γ-TIP mAb 351 (indicated as γ-TIP*, green). A visible light image collected simultaneously in the blue channel is shown in the top left. The different symbols indicate five structures consistent with the appearance of globoids that labeled with both antibodies. (B) Immuno-EM localization of γ-TIP on globoids. Arrows, all gold particles present on the field selected; C, crystalloid. The dark staining material above the globoid to the left represents globoid contents that fell out of the plastic resin and migrated during the staining procedure. Bars: (A) 10 μm; (B) 100 nm.
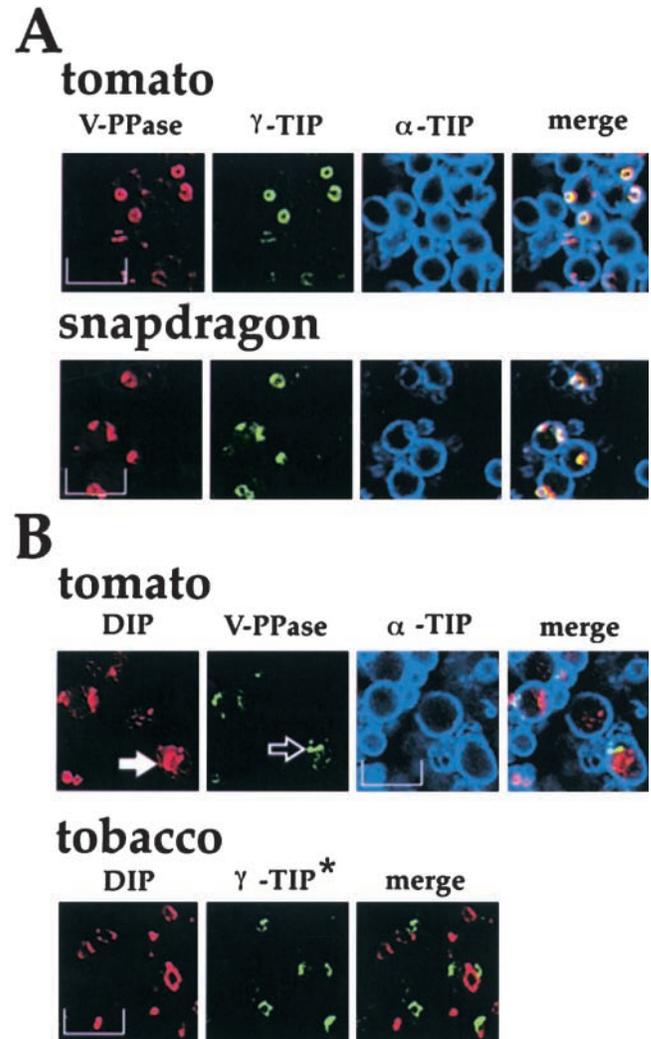


Figure 5.  Localization of V-PPase relative to other proteins in the PSV. (A) Embryo cells in paraffin sections of mature desiccated seeds from tomato (top) or snapdragon (bottom) were labeled with anti–V-PPase protein (red), anti–γ-TIP protein (green), and anti–α-TIP MAb38a (blue) antibodies. (B) Tomato embryo sections (top) were labeled with anti-DIP (red, white arrow), anti–V-PPase protein (green, open arrow), and anti-α-TIP MAb38a antibodies (blue); tobacco embryo sections (bottom) were labeled with anti-DIP (red) and anti–γ-TIP MAb351 (green) antibodies. Bars, 10 μm.

antibody preparations gave the same result argues strongly that the antibodies detected γ-TIP rather than cross-reacting epitopes on other proteins. The fact that the polyclonal anti–γ-TIP peptide antibodies also labeled tonoplast may indicate the presence of a small amount of γ-TIP there or may result from cross-reactivity with other TIPs in tobacco.

### Association with globoids of soluble protein markers for an LV

Taken together, the results argue strongly for the presence of γ-TIP in the globoid membrane. The presence of γ-TIP in the absence of δ-TIP correlates with what we have defined previously as an LV (Jauh et al., 1999). We sought to identify soluble lumenal proteins within the globoid that might be associated with LV functions. Barley aleurain has served as a marker for LVs (Jauh et al., 1999) and has highly con-

served orthologs that are present in other plant species (Rogers et al., 1997). These orthologs share not only the structural features that make aleurain and its mammalian homologue cathepsin H unique among cysteine proteases but also the highly conserved NH$_2$-terminal vacuolar-targeting motif (Rogers et al., 1997). The latter is specifically bound by members of the vacuolar sorting receptor family of which BP-80 is the prototype and directed to the prevacuolar compartment for LVs (Jiang and Rogers, 1998; Di Sansebastiano et al., 2001; Humair et al., 2001). A tobacco ortholog has been identified (Ueda et al., 2000). We used a recombinant protein expressed from this tobacco cDNA on an affinity column to select antibodies from rabbit C serum that cross-reacted with both the barley and tobacco sequences. As shown in Fig. 6 A, left, these antibodies identify a single band of ∼34 kD in tobacco BY-2 cell extract (lane
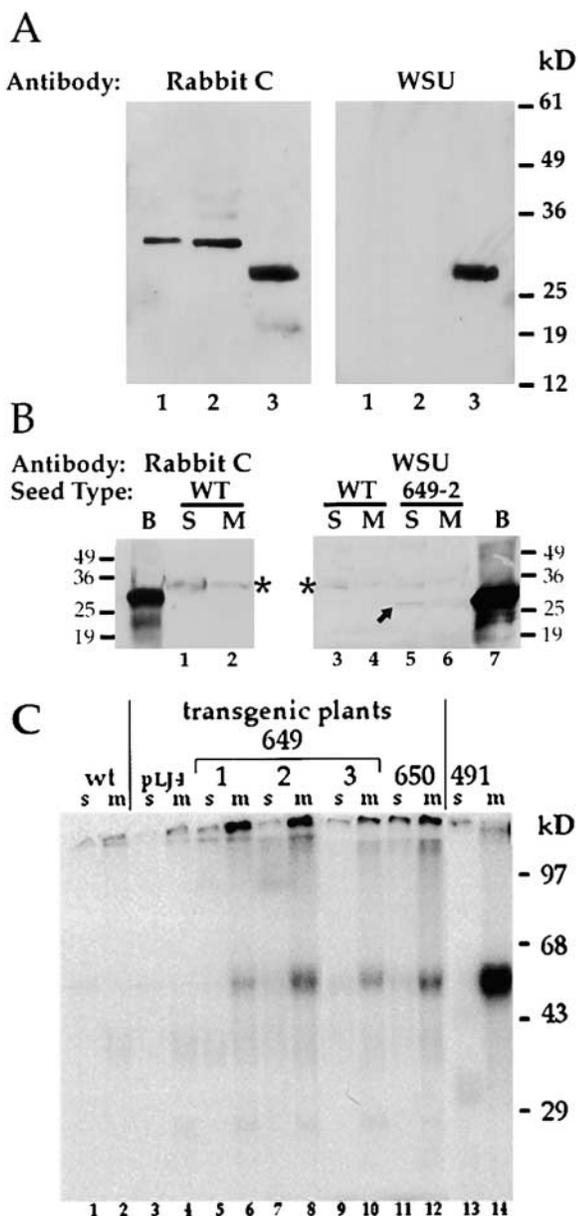
Figure 6. **Identification of a tobacco aleurain-like protein and aleurain derived from a reporter protein in tissue extracts.** (A) Specificity of antialeurain antibodies. 100 μg samples of extracts of BY-2 cells (lane 1), tobacco roots (lane 2), and barley leaves (lane 3) were electrophoresed, transferred to nitrocellulose, and probed with antibodies from rabbit C serum that had been affinity purified on a recombinant tobacco aleurain column (left) or with antibodies from WSU rabbit that had been purified on a recombinant barley aleurain column. (B) Detection of aleurain in seed extracts. Membranes containing electrophoresed 100 μg samples of extracts from barley leaves (B) or from soluble (S) or membrane (M) fractions from mature dry tobacco seeds were probed with antibodies described in A. Seeds were obtained from wild-type plants (lanes 1–4) or from plant 649-2 expressing Re-F-B-B (lanes 5 and 6). Asterisk, position of a tobacco aleurain-like protein; arrow, position of barley aleurain present in the transgenic seed extract. (C) Identification of transgenic plants expressing reporter proteins. From each plantlet grown on agar, 10 root tips ~1 cm in length were labeled with [$^{35}$S]methionine plus cysteine, fractionated into soluble (s) and membrane (m) fractions, and sequentially immunoprecipitated with antialeurain and then anti-FLAG antibodies, and analyzed by SDS-PAGE and autoradiography as described previously (Jiang et al., 2000). The following plants were used: untransformed (wt, lanes 1 and 2), transformed with construct

1), a similar band in tobacco root extract (lane 2), and the ~30-kD barley aleurain band in a barley leaf extract (lane 3). We had previously noted variation in size of aleurain orthologs from different plants and suggested they might result from glycosylation differences (Rogers et al., 1997). (It should also be noted that barley aleurain processed from a reporter protein expressed in tobacco cells runs as a dimer, the larger member of which is ~34 kD [Jiang and Rogers, 1998].) The fact that this ~34-kD tobacco band was recognized by antibodies raised to a *trpE*-barley aleurain fusion that were selected on a tobacco aleurain affinity column argues strongly that it represents a tobacco aleurain-like protein, probably the tobacco aleurain ortholog. In contrast, we found that the WSU antibarley aleurain antibodies in the presence of recombinant tobacco aleurain protein recognized only the ~30-kD barley aleurain protein (Fig. 6 A, right). We used the rabbit C antialeurain antibodies to probe a filter containing proteins from an extract prepared from mature dry tobacco seeds (Fig. 6 B, left). Similar to the results in Fig. 6 A, these antibodies labeled a single band of ~34 kD (asterisk) that was more abundant in the soluble protein fraction (S) than the membrane fraction (M). We concluded that the tobacco aleurain-like protein was present in the soluble fraction of mature seeds.

In a second approach, we generated transgenic plants expressing a chimeric integral membrane reporter protein that traffics to LVs. Re-F-B-B has a lumenal domain comprised of barley proaleurain lacking its vacuolar targeting determinants, which is connected at its COOH terminus to a FLAG epitope tag, which is in turn connected to the transmembrane domain and cytoplasmic tail from the vacuolar sorting receptor, BP-80. Re-F-B-B traffics through the Golgi complex to a lytic prevacuolar compartment where it is proteolytically processed to release soluble aleurain; this processing separates aleurain from the FLAG epitope (Jiang and Rogers, 1998). Under our hypothesis that the globoid is a LV equivalent, we would predict that Re-F-B-B would be directed to that compartment within PSVs.

We identified transgenic plants expressing Re-F-B-B by immunoprecipitating $^{35}$S-labeled proteins sequentially with the original antialeurain antibodies and then with anti-FLAG antibodies from root extracts separated into soluble and membrane fractions (Jiang et al., 2000). This strategy allowed us to detect the ~50-kD full-length integral membrane reporter protein separated from any cross-reactivity the antibodies might have with the ~34 kD soluble endogenous tobacco aleurain ortholog (Rogers et al., 1997); results are presented in Fig. 6 C. Consistent with previous results (Jiang et al., 2000), neither extracts from wild-type plants (Fig. 6 C, lanes 1 and 2) nor from plants transformed with a construct expressing *Escherichia coli* β-glucuronidase (lanes 3 and 4) yielded radioactive bands the size appropriate for the reporter protein (position indicated by arrow). In contrast, in root extracts from three Re-F-B-B gene

pLJ4 expressing *E. coli* β-glucuronidase (lanes 3 and 4), transformed with LJ649 expressing Re-F-B-B (lanes 5–10), and transformed with LJ650 (Jiang et al., 2000) expressing Re-F-B-α. As a standard, extracts from suspension culture protoplasts expressing Re-F-B-B (construct 491; Jiang and Rogers, 1998) and immunoprecipitated with antialeurain antibodies were included in lanes 13 and 14. The positions of molecular weight markers are indicated to the side in each panel.

transformants (649-1, -2, and -3; lanes 6, 8, and 10) and in an extract from a positive control plant expressing Re-F-B-α (650; lane 12) a ~50-kD band was present predominantly in the membrane fraction of each. To confirm the identity of the immunoprecipitated protein, a similar band was immunoprecipitated from the membrane fraction of suspension culture protoplasts transiently expressing Re-F-B-B (construct 491; lane 14). To test for accumulation of the reporter protein in seeds, a filter carrying extracts from wild-type and 649-2 seeds was probed with the WSU antibody. An ~30-kD band similar in size to aleurain in a barley leaf extract (lane 7) was detected in the 649-2 soluble fraction (lane 5, arrow) but not in the wild-type seed fractions. The presence of a faint ~34-kD band (asterisk) of similar intensity in soluble fractions from both wild-type (lane 3) and 649-2 (lane 5) indicates that similar amounts of protein were loaded in each and that the presence of the ~30-kD band in 649-2 represents aleurain processed from Re-F-B-B and accumulated in the transgenic seed.

We used confocal immunofluorescence to localize the aleurain-like protein in wild-type (nontransformed) seeds. As shown in Fig. 7 A, the antialeurain antibodies from rabbit C (red) colocalized with anti–γ-TIP MAb351 (green) that served as the globoid marker. When the fluorescent images were superimposed upon a visible light image collected simultaneously in the blue channel (left), consistent with results shown in Fig. 4, they labeled globoids (arrows). In contrast, when the barley aleurain-specific antibodies from WSU antiserum were used on sections from wild-type seeds, essentially no labeling above background was obtained (Fig. 7 B, red), whereas MAb351 labeling of globoids (Fig. 7 B, green) was similar to that in Fig. 7 A. When seeds from transgenic plant 649-2 expressing the Re-F-B-B reporter protein were studied, strong labeling with the WSU antialeurain antibodies was obtained (Fig. 7 C, red), which colocalized with MAb351 (green) on globoids. The tissue samples used in labeling studies shown in Fig. 7, A–C, were fixed, processed, and labeled with antibodies concurrently, and the images were collected during the same microscopy session using identical parameters for each. We conclude that the WSU antialeurain antibodies are specific for barley aleurain associated with the reporter protein expressed from the transgene and that both the endogenous tobacco aleurain-like protein and the reporter protein were associated specifically with globoids. The fact that labeling for aleurain was present in a ring similar to γ-TIP labeling on the globoid membrane would be explained if formation of the phytic acid crystal within the globoid displaced soluble proteins to the periphery.

In a separate set of experiments, we tested whether the barley aleurain epitopes were together with the FLAG epitope in the globoid. When embryos from seeds from a transgenic tobacco plant expressing Re-F-B-B were studied, antialeurain antibodies colocalized with V-PPase (Fig. 7 D); however, no FLAG labeling was obtained (Fig. 7 E). As a control, in embryos from a plant expressing Re-F-B-α, antialeurain antibodies labeled crystalloid and were separate from V-PPase (Fig. 7 F) but colocalized with FLAG (Fig. 7 G) as shown previously (Jiang et al., 2000). We concluded that in transgenic tobacco seeds Re-F-B-B traffics to the globoid cavity on a pathway where the aleurain epitopes are separated from the FLAG epitope.
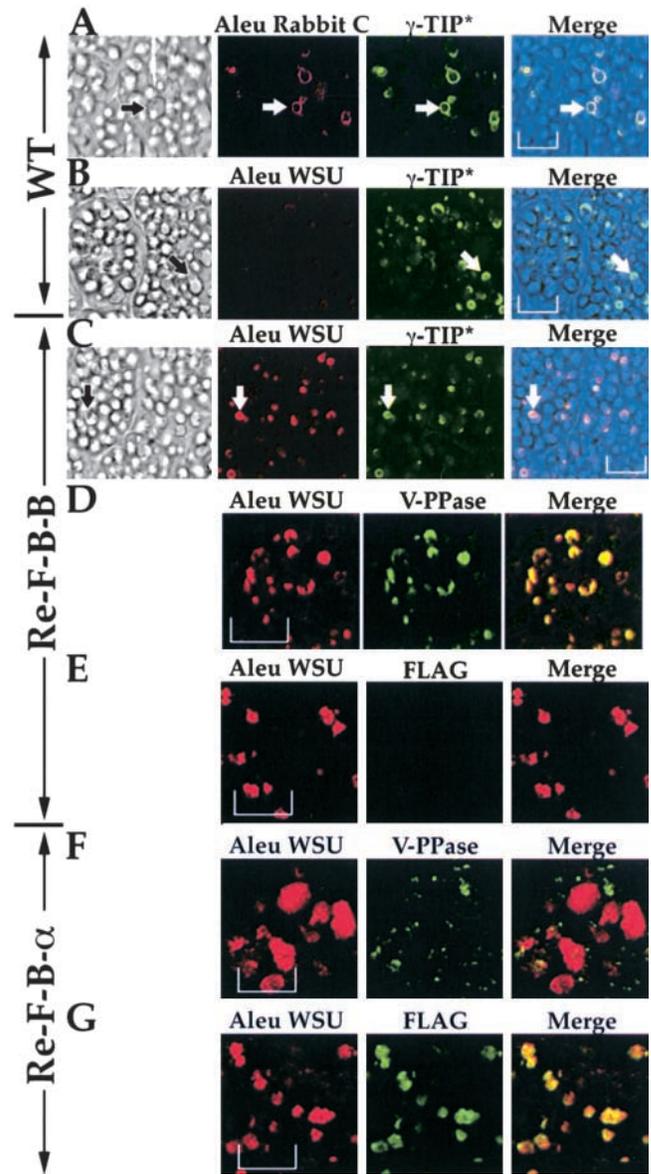


Figure 7. **Localization of aleurain-like protein and aleurain in tobacco embryo PSVs.** (A) Mature desiccated seed section from a wild-type plant was labeled with antialeurain antibodies from rabbit C (red) and anti–γ-TIP MAb351 (green). (B) Similar section labeled with antibarley aleurain-specific WSU antibodies (red) and MAb351 (green). (C) Section from 649-2 transgenic seed expressing Re-F-B-B labeled as in B. Section as in B were labeled with WSU antialeurain (red) and anti–V-PPase protein (green) antibodies (D) or with WSU antialeurain and anti-FLAG monoclonal (green) antibodies (E). (F) Seed from a plant expressing Re-F-B-α; antibody designations as in D. (G) Antibody designations as in E. The images in A–C were from sections prepared and labeled in the same experiment in an identical manner for each; images were collected sequentially in the same session using identical conditions for each sample. Arrows in A–C indicate examples of visibly identifiable globoids that labeled with both antibodies. Bars, 10 μm.

## Aleurain colocalizes with a marker for multivesicular body prevacuolar organelles

We searched for labeling with the two different antialeurain antibodies in developing seeds in an attempt to identify a prevacuolar compartment that contributed to
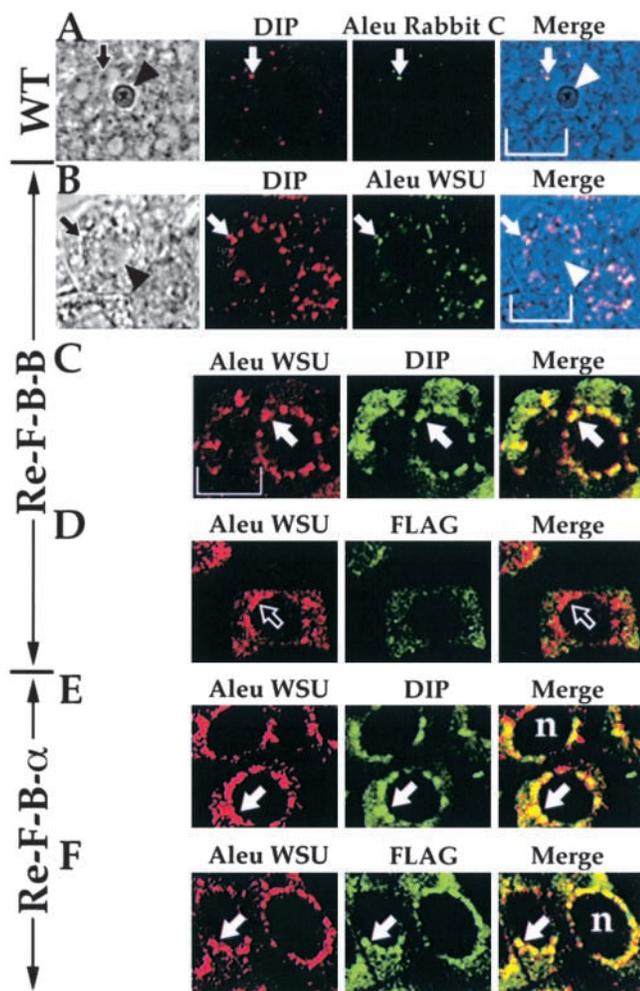
Figure 8. **Colocalization of tobacco aleurain-like protein and reporter proteins with DIP.** (A) Developing seeds from a wild-type plant were collected at ~12 d after pollination and processed for microscopy. Sections were labeled with anti-DIP (red) and rabbit C antialeurain (green) antibodies. (B) Developing seeds from progeny of the 649-2 transgenic plant expressing Re-F-B-B were harvested and sections labeled as in A except WSU antibarley aleurain antibodies were used. Arrows in both indicate examples of organelles labeled with both antibodies, whereas arrowheads indicate the positions of the nuclei in the two cells. (C–F) Root tip cells were prepared from each plant and labeled with antibodies under identical conditions in the same experiment; confocal images were obtained sequentially in the same session under identical conditions for each set. Solid arrows indicate organelles labeled with both antibodies in a given comparison; open arrows indicate organelles labeled only with antialeurain antibodies. Arrows are placed over the positions of the cell nuclei (n). (C) Cells expressing Re-F-B-B labeled with antialeurain (red) and anti-DIP (green) antibodies (top) or anti-aleurain (red) and anti-FLAG monoclonal antibodies (green) (D). (E) Cells expressing Re-F-B-α labeled as in C. (F) Cells expressing Re-F-B-α labeled as in D. Note the bar in C applies to C–F. Bar, 10 μm.

globoid formation. We found that both labeling for the endogenous tobacco aleurain-like protein in wild-type seeds (Fig. 8 A, green) and for the aleurain epitopes associated with Re-F-B-B (Fig. 8 B, green) colocalized with the TIP DIP on small punctate structures in cells from seeds collected at ~12 d after pollination. These structures were indistinguishable from prevacuolar organelles identified

previously in developing seeds by their labeling for DIP (Jiang et al., 2000).

Similar structures were also previously found to be present in some root tip cells where they also were taken up into vacuoles labeled for α-TIP, a marker for PSVs (Jiang et al., 2000). Here, in transgenic tobacco root tip cells expressing Re-F-B-B the reporter protein as detected with antialeurain antibodies colocalized with DIP on cytoplasmic organelles ~1–2 μm in diameter (Fig. 8 C), but labeling for the FLAG epitope was not detected (Fig. 8 D). In comparison, in transgenic tobacco root tip cells expressing Re-F-B-α antialeurain antibodies colocalized with DIP on similar structures (Fig. 8 E), but differing from the results obtained for Re-F-B-B, aleurain and FLAG epitopes were present together in the same organelles (Fig. 8 F). Thus, results from both developing seeds and root tips are consistent for both reporter proteins. In Re-F-B-α–expressing plants, essentially all of these cytoplasmic DIP organelles contain the reporter protein (Jiang et al., 2000). Although we have not been able to compare the two reporter proteins expressed together in one plant, it is likely that the same cytoplasmic prevacuolar organelles would contain both reporter proteins. We propose an hypothesis below to explain how this could occur.

## Discussion

Electron microscopists who study plants have argued for more than 30 years about whether a membrane surrounds the globoid cavity. There have been two central arguments against that possibility. First, standard transmission EM and freeze-fracture studies have not demonstrated a membrane, and second there was no known mechanism by which an internal membrane-bound structure within a vacuole could be generated (Weber and Neumann, 1980). These two points are addressed sequentially as follows.

The absence of microscopic evidence was relative rather than absolute. Some studies using standard osmium fixation protocols, particularly in systems where developing PSVs were present, showed osmiophilic structures surrounding globoid cavities that would be consistent with the appearance of membranes (Jones and Price, 1970; Monma et al., 1992; Krasowsky and Owens, 1993). However, these studies did not show a unit membrane structure, and it was possible that the osmiophilic structures resulted from dense compression of proteins. Additionally, freeze-fracture studies of globoids in dicotyledonous plant seeds did not demonstrate a cleavage plane at the globoid PSV interface that would be expected if a membrane surrounded the phytic acid crystals (Lott, 1980; Spitzer and Lott, 1980). However, other studies using cereal grains did demonstrate such a cleavage plane (Buttrose, 1971; Swift and Buttrose, 1972; Fernandez and Staehelin, 1985), although it was noted that the appearance of the interface layer differed from that of other membranes in the cell (Fernandez and Staehelin, 1985).

The lipid composition of a globoid membrane could differ substantially from that of the PSV tonoplast. For example, in mammalian cells internal membranes in multivesicular body late endosomes contain abundant lysobisphosphatidic acid (Kobayashi et al., 1998). Additionally, the fact

that these results were derived from dry seeds in which a potential globoid membrane would have been desiccated onto the surface of a crystal of inositol hexaphosphate raises the possibility that such a membrane might have different physical characteristics than a tonoplast or plasma membrane, characteristics that could affect freeze fracture and staining with osmium. The staining characteristics of such a membrane would be unpredictable, and it is clear that developmental changes in lipid composition can greatly affect staining after treatment with osmium. For example, during oogenesis in the fern *Paesia* plastid envelopes become progressively less distinct after aldehyde fixation and osmication, but reaction to permanganate is unchanged; this phenomenon is due to a specific change in plastid membrane lipids because mitochondrial envelopes remain unchanged throughout oogenesis (Bell, 1983).

Our results with permanganate fixation to demonstrate a unit membrane boundary between globoid and PSV matrix are relevant in this regard: extensive treatment with permanganate resulted in loss of visible PSV tonoplast but maintained the globoid membrane. Since permanganate is known to react specifically with membrane lipids, especially phospholipids (Ongun et al., 1968), this difference may have resulted from different lipid compositions and lipid/protein ratios within globoid versus tonoplast membranes.

There are solid precedents for internal membrane-bound compartments within vacuoles. The intravacuolar chambers that contain calcium oxalate crystals are clearly defined by unit membranes (Arnott and Pautard, 1970), and formation of the chambers is preceded by the presence of abundant membrane vesicles within the vacuole (Franceschi, 1984). Additionally, when anthocyanins are produced in sweet potato suspension culture cells they are deposited in intravacuolar pigmented globules. A soluble metalloprotease, VP24, which is proteolytically processed from a 96-kD precursor that has multiple transmembrane domains, accumulates to high levels in the globules (Xu et al., 2001). The COOH-terminal portion of the 96-kD precursor was also localized to the intravacuolar globules and not the vacuole tonoplast (Xu et al., 2000). Interestingly, as judged by neutral red accumulation the globules are acidic, whereas the surrounding central vacuole is less so or not at all (Nozue et al., 1993; Kubo et al., 1995). Thus the globules are likely to be surrounded by a membrane.

These intravacuolar compartments must exist for the same reasons separate membrane-bound organelles exist within the secretory pathway: they define a specialized environment that is required for certain functions without interference from ongoing processes in other organelles. In the case of the globoid cavity, we hypothesize that the internal environment is optimal for formation of phytic acid crystals. The facts that the globoid membrane contains a pyrophosphate-driven proton pump, V-PPase, and that phytic acid molecules are known to carry pyrophosphate groups (Loewus and Murthy, 2000) raises the interesting possibility that the association of the two in the globoid may have functional significance. However, interpretation of this association is complicated by the fact that the orientation of the V-PPase protein in the globoid membrane is not known. Additionally, our finding that the globoid membrane contains γ-TIP, which is

a marker for LVs, and that a marker for the LV pathway, Re-F-B-B, traffics to it together argue that the globoid represents an internal LV-like compartment. The globoid membrane would thus separate the storage compartment outside from potentially deleterious lytic functions inside. Our results indicate that a tobacco aleurain-like protein, possibly the tobacco ortholog of aleurain, is normally present in the globoid. It will be helpful to learn if other digestive enzymes are also present. In future studies, it will be important to follow the fate of globoid cavities within PSVs early during seed germination to learn if the globoid contents gain access to the storage compartment and participate in their breakdown.

Our results demonstrate that a PSV is the equivalent of a large multivesicular body. How does the internal globoid cavity originate? One possibility is that the globoid cavity represents a preformed LV that is then taken up into the developing PSV by autophagy, perhaps during the process by which enlarging PSVs displace preexisting LVs during seed development (Hoh et al., 1995). Such a process should result in a double membrane around the internalized structure, but our micrographs demonstrated only a single unit membrane around the globoid, an observation that would argue against a process involving autophagy (Teter and Klionsky, 2000). However we cannot exclude the possibility that one of the double membranes could have been removed by a digestive process after internalization. Alternatively, our localization of two different reporter proteins in transgenic plants to what appear to be the same prevacuolar organelles provides the basis for hypothesizing a different mechanism (Jiang and Rogers, 2001). We demonstrated previously that the contents of multivesicular prevacuolar organelles are taken up by PSVs during PSV development and internal membrane-containing structures in the organelles then assemble into the PSV crystalloid (Jiang et al., 2000). We would postulate that the globoid compartment would be formed from a separate membrane-defined compartment within the prevacuolar organelles (Jiang and Rogers, 2001). Such a mechanism would be consistent with the observation in developing castor bean endosperm that phytic acid was present within small cytoplasmic structures having the appearance of multivesicular bodies that appeared to be transported to the PSV where the phytic acid was taken up and assembled into the globoid (Greenwood and Bewley, 1984). This alternative model is limited by lack of information as to how a multivesicular body prevacuolar organelle could incorporate lytic enzymes selectively into its internal vesicles, but that is essentially the same question posed by the presence of lytic enzymes inside the membrane-bounded globoid cavity.

A final point should be emphasized. These studies provide the first demonstration that V-PPase may be present on a specific membrane type associated with a plant vacuole, a finding that indicates V-PPase may be required for special vacuole functions. This observation is so far limited specifically to cells in seed embryos because in other experiments we found that anti–V-PPase antibodies labeled all vacuoles in root tip cells (Jauh et al., 1999; Jiang et al., 2000). A contribution by V-PPase to specific functions presumably would explain why, in apicomplexian parasites such as trypanosomes and *Leish-*

*mania*, H$^+$-ATPase is present in the lysosome-like vacuole membrane, whereas V-PPase is present in the membrane of acidocalciosomes, which are acidic vacuoles that concentrate calcium (Scott et al., 1998; Rodrigues et al., 1999).

## Materials and methods

Methods for tissue preparation, wide-field and confocal immunofluorescence microscopy, controls to assess specificity of double-labeling procedures, characterization of affinity-purified polyclonal antibodies against DIP (Culianez-Macia and Martin, 1993), α-, δ-, and γ-TIP, characterization of mouse monoclonal anti–γ-TIP MAb351 and anti–α-TIP Mab38a, and commercial sources for anti-FLAG antibodies have all been described (Jauh et al., 1999; Jiang et al., 2000).

### Antibodies

Monoclonal antibody IgM38 was obtained incidentally during the screen for anti–α-TIP antibodies; this cross-reacts with an unknown protein in tomato PSV matrix and serves as a matrix marker. Antipeptide antisera were raised in rabbits to sequences from V-PPase proteins: peptide 324, sequence TKAADVGADLVGKIE in putative hydrophilic loop III of Arabidopsis V-PPase (AVP)1 (Sarafian et al., 1992); peptide 1368, sequence EEG-VNDQSVVAKCAE of putative hydrophilic loop I of AVP1; and peptide 1401, sequence KGTRDASVKSPVED of putative hydrophilic loop IV of AVP2 (Drozdowicz et al., 2000). These antisera were used at a dilution of 1:100. Transgenic tobacco plants expressing Re-F-B-B were generated and characterized in a manner identical to that described for Re-F-B-α–expressing plants (Jiang et al., 2000).

Two different antisera were used to prepare affinity-purified antialeurain antibodies. (a) Antiserum from one of two rabbits immunized with a gel-purified *trpE*-aleurain fusion protein (Holwerda et al., 1990); this is referred to as rabbit C antiserum. (It should be noted that antibodies from rabbit B antiserum were used to immunoprecipitate proteins in transient expression experiments [Holwerda et al., 1992; Jiang and Rogers, 1998].) (b) Antiserum raised to a His-tagged recombinant aleurain (Rogers et al., 1997); this is referred to as the WSU antiserum. A cDNA clone for the tobacco ortholog of barley aleurain, NTCP-23 (Ueda et al., 2000), was provided by Dr. T. Ueda (National Institute of Agrobiological Resources, Tsukuba, Japan). A His-tagged recombinant protein representing nucleotides 461–1117 was expressed in *E. coli*, purified, and coupled to agarose as described previously for barley aleurain (Rogers et al., 1997). Affinity-purified antibodies from the WSU antiserum were prepared using the recombinant barley aleurain affinity column (Rogers et al., 1997), whereas antibodies were purified from the rabbit C antiserum using the tobacco aleurain column. To further limit the specificity of the WSU antibodies to barley aleurain, they were absorbed with acetone powder (Harlow and Lane, 1988) prepared from tobacco BY-2 suspension culture cells before use in immunofluorescence experiments.

### Fractionation of PSVs

Fractions enriched in tonoplast, crystalloid, and globoid were prepared from PSVs isolated from mature dry tomato seeds homogenized in glycerol as described previously for pumpkin PSVs (Jiang et al., 2000) with slight modifications. Sucrose solutions were made per cent wt:wt (Youle and Huang, 1976), and tonoplast was collected from the top of the 30% cushion, crystalloid from the 68% cushion, and purified globoids from the pellet at the bottom of the tube. In an alternative protocol, to minimize possible loss of membrane from the surface of globoids purified PSVs in glycerol were diluted to 80% glycerol with 10 mM Tris-HCl, pH 8, and 1 mM EDTA and mixed with a vortex mixer vigorously at room temperature over a 10-min period. The entire suspension was then layered over a cushion of CCl$_4$ and centrifuged at 4,000 *g* for 10 min. The supernate was removed and saved, and the interface was then extracted four times by resuspending it in 80% glycerol. The supernates after each centrifugation were saved and pooled. Material collected at the interface after the final wash was defined as globoid because it had a density sufficient to allow it to pellet from 80% glycerol at 4,000 *g*. Material in the pooled supernates was collected by centrifugation at 10,000 *g* after dilution to a final glycerol concentration of 25% and was defined as tonoplast plus crystalloid.

### EM

For transmission EM, dry tobacco seeds were initially fixed overnight at room temperature in 2% freshly depolymerized paraformaldehyde and 2.5% glutaraldehyde in 70 mM NaCl, 30 mM Hepes, and 2 mM CaCl$_2$, pH

7.4, after slicing off the top and bottom 10–20% of the seed to allow better penetration of the fixative. At this point, additional dissection of the seed with a razor blade resulted in easy separation of the embryo from the surrounding seed coat. The embryo was then fixed for an additional 2 h in the same fixative, rinsed three times in distilled water, and post-fixed in either 0.5 or 2.5% potassium permanganate for 2 h at room temperature. After extensive rinsing with water, the tissues were stained en bloc in alkaline bismuth at 40°C for 30 min (Park et al., 1988) before being rinsed in water and dehydrated with an ethanol series. The tissue was infiltrated slowly with an epoxy resin (EmBed 812; Electron Microscopy Sciences). Ultra thin sections were either viewed without further staining or counter stained with uranyl acetate and lead citrate and examined with a JEOL 1200 EX transmission electron microscope.

For immunocytochemistry, mature dry tomato seeds were fixed in 2% freshly depolymerized paraformaldehyde after having the apex and base of their seed coat cut off using a razor blade. After 2 h in the fixative, the seeds were further dissected under a stereoscope to free the cotyledons. After an additional 2 h in fixative, the cotyledons were rinsed en bloc, stained with 0.5% uranyl acetate in ethanol or 25% ethanol for 1 h, and dehydrated with an ethanol series (25, 50, 70, 90, and 3 × 100%) for 10 min each before being infiltrated with LR Gold resin (Electron Microscopy Sciences). Silver sections were picked up on 600 mesh nickel grids, and nonspecific binding sites were blocked by immersion in blocking buffer (BB; 70 mM NaCl, 30 mM Hepes, 0.1% Tween 20, 1% normal goat serum, 0.8% BSA, 0.2% ovalbumin, 0.1% microprotect [Boehringer-Mannheim]) for 1–15 h. The sections were next immersed in 20–40 μl drops of primary monoclonal antibody 351 diluted 1:2,000 in BB for 15 h. After extensive rinsing, the sections were incubated in a goat anti–mouse immunoglobulin secondary antibody conjugated to 12 nm colloidal gold (Jackson ImmunoResearch Laboratories) diluted 1:40 in BB for 4 h. After rinsing, the sections were counterstained with uranyl acetate and lead citrate. For quantitative studies, randomly chosen globoid cavities were photographed at 40,000 *g*. In a sandwich immunocytochemical-staining protocol, the colloidal gold particle can be separated from the target antigen by the size of the gold particle plus the 8–10 nm extended length of both the primary and secondary IgG molecules (Griffiths, 1993). Thus, in our studies any gold particle within a 30-nm radius of the target membrane was counted as specifically bound. The photomicrographs were converted to digital images by high resolution scanning and Adobe Photoshop® used to draw a 60-nm-wide band centered over the outer edge of the globoid cavity or tonoplast membrane. For the crystalloid, the total area of the crystalloid, extending 30 nm outside of its outer edges, was counted. In a small number of cases when two of these regions were closely apposed, a gold particle was located in an area such that it could be counted as belonging to either region. These "double counted" gold particles were <5% of all particles counted. For counting purposes, the location of gold particles was determined by visual inspection of the photographic negatives placed on a light box, since subtle differences in the densities of the globoid contents and colloidal gold could be unequivocally discerned by eye but were sometimes difficult to perceive on the digitized images. The number of gold particles counted was expressed relative to the surface area measured. Statistical analysis of the data was performed using a two-group unpaired Mann-Whitney U-test.

## References

Arnott, H.J., and F.G.E. Pautard. 1970. Calcification in plants. *In* Biological Calcification: Cellular and Molecular Aspects. H. Schraer, editor. Appleton-

Century-Crofts, New York. 375–446.

Bell, P.R. 1983. Plastid envelopes in reproductive cells. *Eur. J. Cell Biol.* 30:279–282.

Buttrose, M.S. 1971. Ultrastructure of barley aleurone cells as shown by freeze etching. *Planta.* 96:13–26.

Culianez-Macia, F.A., and C. Martin. 1993. DIP: a member of the MIP family of membrane proteins that is expressed in mature seeds and dark-grown seedlings of *Antirrhinum majus. Plant J.* 4:717–725.

Di Sansebastiano, G.P., N. Paris, S. Marc-Martin, and J.-M. Neuhaus. 1998. Specific accumulation of GFP in a non-acidic vacuolar compartment via a C-terminal propeptide-mediated sorting pathway. *Plant J.* 15:449–457.

Di Sansebastiano, G.-P., N. Paris, S. Marc-Martin, and J.-M. Neuhaus. 2001. Regeneration of a lytic central vacuole and of neutral peripheral vacuoles can be visualized by green fluorescent proteins targeted to either type of vacuoles. *Plant Physiol.* 126:78–86.

Drozdowicz, Y.M., J.C. Kissinger, and P.A. Rea. 2000. AVP2, a sequence-divergent, K$^+$-insensitive H$^+$-translocating inorganic pyrophosphatase from Arabidopsis. *Plant Physiol.* 123:353–362.

Fernandez, D.E., and L.A. Staehelin. 1985. Structural organization of ultrarapidly frozen barley aleurone cells actively involved in protein secretion. *Planta.* 165:455–468.

Franceschi, V.R. 1984. Developmental features of calcium oxalate crystal sand deposition in *Beta vulgaris* L. leaves. *Protoplasma.* 120:216–223.

Greenwood, J.S., and J.D. Bewley. 1984. Subcellular distribution of phytin in the endosperm of developing castor bean: a possibility for its synthesis in the cytoplasm prior to deposition within protein bodies. *Planta.* 160:113–120.

Griffiths, G. 1993. Fine Structure Immunocytochemistry. Springer-Verlag, Berlin, Germany. 459 pp.

Hara-Nishimura, I., T. Shimada, K. Hatano, Y. Takeuchi, and M. Nishimura. 1998. Transport of storage proteins to protein storage vacuoles is mediated by large precursor-accumulating vesicles. *Plant Cell.* 10:825–836.

Higuchi, T., S. Suga, T. Tsuchiya, H. Hisada, S. Morishima, Y. Okada, and M. Maeshima. 1998. Molecular cloning, water channel activity and tissue specific expression of two isoforms of radish vacuolar aquaporin. *Plant Cell Physiol.* 39:905–913.

Hinz, G., S. Hillmer, M. Bäumer, and I. Hohl. 1999. Vacuolar storage proteins and the putative sorting receptor BP-80 exit the Golgi apparatus of developing pea cotyledons in different transport vesicles. *Plant Cell.* 11:1509–1524.

Hoh, B., G. Hinz, B.-K. Jeong, and D.G. Robinson. 1995. Protein storage vacuoles form de novo during pea cotyledon development. *J. Cell Sci.* 108:299–310.

Holwerda, B.C., N.J. Galvin, T.J. Baranski, and J.C. Rogers. 1990. In vitro processing of aleurain, a barley vacuolar thiol protease. *Plant Cell.* 2:1091–1106.

Holwerda, B.C., H.S. Padgett, and J.C. Rogers. 1992. Proaleurain vacuolar targeting is mediated by short contiguous peptide interactions. *Plant Cell.* 4:307–318.

Humair, D., D. Hernández Felipe, J.-M. Neuhaus, and N. Paris. 2001. Demonstration in yeast of the function of BP-80, a putative plant vacuolar sorting receptor. *Plant Cell.* 13:781–792.

Jauh, G.-Y., T. Phillips, and J.C. Rogers. 1999. Tonoplast intrinsic protein isoforms as markers for vacuole functions. *Plant Cell.* 11:1867–1882.

Jiang, L., and J.C. Rogers. 1998. Integral membrane protein sorting to vacuoles in plant cells: evidence for two pathways. *J. Cell Biol.* 143:1183–1199.

Jiang, L., and J.C. Rogers. 2001. Compartmentation of proteins in the protein storage vacuole, a compound organelle in plant cells. *Adv. Bot. Res.* 35:139–173.

Jiang, L., T.E. Phillips, S.W. Rogers, and J.C. Rogers. 2000. Biogenesis of the protein storage vacuole crystalloid. *J. Cell Biol.* 150:755–769.

Jones, R.L., and J.M. Price. 1970. Gibberellic acid and the fine structure of barley aleurone cells. III. Vacuolation of the aleurone cell during the phase of ribonuclease release. *Planta.* 94:191–202.

Kobayashi, T., E. Stang, K.S. Fang, P. de Moerloose, R.G. Parton, and J. Gruenberg. 1998. A lipid associated with the antiphospholipid syndrome regulates endosome structure and function. *Nature.* 392:193–197.

Krasowsky, M.J., and J.N. Owens. 1993. Ultrastructural and histochemical postfertilization megagametophyte and zygotic embryo development of white spruce (*Picea glauca*) emphasizing the deposition of seed storage products. *Can. J. Bot.* 71:98–112.

Kubo, H., M. Nozue, K. Kawasaki, and H. Yasuda. 1995. Intravacuolar spherical bodies in *Polygonum cuspidatum. Plant Cell Physiol.* 36:1453–1458.

Harlow, E., and D. Lane. 1988. Antibodies: A Laboratory Manual. Cold Spring Harbor Laboratory, Cold Spring Harbor, NY. 726 pp.

Loewus, F.A., and P.P.N. Murthy. 2000. *myo*-inositol metabolism in plants. *Plant Sci.* 150:1–19.

Lott, J.N.A. 1980. Protein bodies. *In* The Biochemistry of Plants. Vol. 1. N.E. Tolbert, editor. Academic Press, New York. 589–623.

Maeshima, M. 1992. Characterization of the major integral protein of vacuolar membrane. *Plant Physiol.* 98:1248–1254.

Maeshima, M., and S. Yoshida. 1989. Purification and properties of vacuolar membrane proton-translocating inorganic pyrophosphatase from mung bean. *J. Biol. Chem.* 264:20068–20073.

Meek, G.A. 1976. Practical Electron Microscopy for Biologists. John Wiley & Sons, Inc., London. 528 pp.

Monma, M., T. Sugimoto, K. Hashizume, and K. Saio. 1992. Biogenesis of protein bodies in embryonic axes of soybean seeds (*Glycine max cv. Enrei*). *Biosci. Biotech. Biochem.* 56:1036–1040.

Nozue, M., H. Kubo, M. Nishimura, A. Katou, C. Hattori, N. Usuda, T. Nagata, and H. Yasuda. 1993. Characterization of intravacuolar pigmented structures in anthocyanin-containing cells of sweet potato suspension culture cells. *Plant Cell Physiol.* 34:803–808.

Ongun, A., W.W. Thomson, and J.B. Mudd. 1968. Lipid fixation during preparation of chloroplasts for electron microscopy. *J. Lipid Res.* 9:416–424.

Paris, N., C.M. Stanley, R.L. Jones, and J.C. Rogers. 1996. Plant cells contain two functionally distinct vacuolar compartments. *Cell.* 85:563–572.

Park, P., T. Ohno, Y. Kawa, and S. Manabe. 1988. Alkaline bismuth solution as an en bloc stain for formaldehyde-glutaraldehyde potassium permanganate fixed fungal spores. *Stain Technol.* 63:229–234.

Rodrigues, C.O., D.A. Scott, and R. Docampo. 1999. Presence of a vacuolar H$^+$-pyrophosphatase in promastigotes of *Leishmania donovani* and its localization to a different compartment from the vacuolar H$^+$-ATPase. *Biochem. J.* 340:759–766.

Rogers, S.W., M. Burks, and J.C. Rogers. 1997. Monoclonal antibodies to barley aleurain and homologues from other plants. *Plant J.* 11:1359–1368.

Sarafian, V., Y. Kim, R.J. Poole, and P.A. Rea. 1992. Molecular cloning and sequence of cDNA encoding the pyrophosphate-energized vacuolar membrane proton pump of *Arabidopsis thaliana. Proc. Natl. Acad. Sci. USA.* 89:1775–1779.

Scott, D.A., W. de Souza, M. Benchimol, L. Zhong, H.-G. Lu, S.N.J. Moreno, and R. Docampo. 1998. Presence of a plant-like proton-pumping pyrophosphatase in acidocalcisomes of *Trypanosoma cruzi. J. Biol. Chem.* 273:22151–22158.

Spitzer, E., and J.N.A. Lott. 1980. Thin-section, freeze-fracture, and energy dispersive x-ray analysis studies of the protein bodies of tomato seeds. *Can. J. Bot.* 58:699–711.

Swift, J.G., and M.S. Buttrose. 1972. Freeze-etch studies of protein bodies in wheat scutellum. *J. Ultrastr. Res.* 40:378–390.

Teter, S.A., and D.J. Klionsky. 2000. Transport of proteins to the yeast vacuole: autophagy, cytoplasm-to-vacuole targeting, and role of the vacuole in degradation. *Sem. Cell Dev. Biol.* 11:173–179.

Ueda, T., S. Seo, Y. Ohashi, and J. Hashimoto. 2000. Circadian and senescence-enhanced expression of a tobacco cysteine protease gene. *Plant Mol. Biol.* 44:649–657.

Weber, E., and D. Neumann. 1980. Protein bodies, storage organelles in plant seeds. *Biochem. Physiol. Pflanzen.* 175:279–306.

Xu, W., K. Moriya, K. Yamada, M. Nishimura, H. Shioiri, M. Kojima, and M. Nozue. 2000. Detection and characterization of a 36-kDa peptide in C-terminal region of a 24-kDa vacuolar protein (VP24) precursor in anthocyanin-producing sweet potato cells in suspension culture. *Plant Sci.* 160:121–128.

Xu, W., H. Shioiri, M. Kojima, and M. Nozue. 2001. Primary structure and expression of a 24-kD vacuolar protein (VP24) precursor in anthocyanin-producing cells of sweet potato in suspension culture. *Plant Physiol.* 125:447–455.

Youle, R.J., and A.H.C. Huang. 1976. Protein bodies from the endosperm of castor bean. *Plant Physiol.* 58:703–709.

Zhen, R.-G., E.J. Kim, and P.A. Rea. 1997. The molecular and biochemical basis of pyrophosphate-energized proton translocation at the vacuolar membrane. *Adv. Bot. Res.* 25:298–337.